

**SAE TECHNICAL
PAPER SERIES**

2008-01-0953

Developing a 10cc Single-Valve, Reverse Uniflow, 2S Engine

Colin B. Bosman and S. Scott Goldsborough
Marquette University

Reprinted From: **Multi-Dimensional Engine Modeling, 2008**
(SP-2171)

ISBN 978-0-7680-1639-0



9 780768 016390

SAE *International*[™]

2008 World Congress
Detroit, Michigan
April 14-17, 2008

By mandate of the Engineering Meetings Board, this paper has been approved for SAE publication upon completion of a peer review process by a minimum of three (3) industry experts under the supervision of the session organizer.

All rights reserved. No part of this publication may be reproduced, stored in a retrieval system, or transmitted, in any form or by any means, electronic, mechanical, photocopying, recording, or otherwise, without the prior written permission of SAE.

For permission and licensing requests contact:

SAE Permissions
400 Commonwealth Drive
Warrendale, PA 15096-0001-USA
Email: permissions@sae.org
Tel: 724-772-4028
Fax: 724-776-3036



For multiple print copies contact:

SAE Customer Service
Tel: 877-606-7323 (inside USA and Canada)
Tel: 724-776-4970 (outside USA)
Fax: 724-776-0790
Email: CustomerService@sae.org

ISSN 0148-7191

Copyright © 2008 SAE International

Positions and opinions advanced in this paper are those of the author(s) and not necessarily those of SAE. The author is solely responsible for the content of the paper. A process is available by which discussions will be printed with the paper if it is published in SAE Transactions.

Persons wishing to submit papers to be considered for presentation or publication by SAE should send the manuscript or a 300 word abstract of a proposed manuscript to: Secretary, Engineering Meetings Board, SAE.

Printed in USA

Developing a 10cc Single-Valve, Reverse Uniflow, 2S Engine

Colin B. Bosman and S. Scott Goldsborough
Marquette University

Copyright © 2008 SAE International

ABSTRACT

A 10cc single-valve, reverse uniflow 2S engine is being developed to power a compact compressor system; the output from this device could be hydraulic or pneumatic power. In this design a free piston is used to directly compress the power fluid. In the initial configuration fresh charge will be delivered through a single, dual-acting spring-loaded poppet valve located in the center of the cylinder and the burned charge is exhausted through symmetrically-arranged ports located at the bottom section of the cylinder; two combustion chambers exist on opposite ends of the piston. Of particular interest in the early stages of the engine development is the gas transfer system; proper cylinder scavenging is required to ensure adequate engine operation. An initial design is being investigated using the commercial computational fluid dynamics software suite, STAR-CD/ESICE. This report will document some initial simulations and indicate areas requiring further refinement. Unique features of the reverse-flow arrangement are highlighted

INTRODUCTION

A novel, reverse uniflow two-stroke (2S) engine is being developed to power a compact compressor system; the output from this portable device could be hydraulic or pneumatic power. Personal-size devices are envisioned but the configuration could be extrapolated to large sizes for automotive type applications. The preliminary design utilizes a free piston to directly compress the working fluid. Free piston geometries have received significant attention in recent years as alternatives to crankshaft driven configurations [1-10]. Multiple arrangements are possible; one considered here utilizes combustion at alternating ends of the device to drive a single piston back and forth; the power fluid will be compressed in an annular region of the oscillating piston. On the gas-side, fresh charge is compressed in one of the combustion chambers while burned charge is expanded in another. The fresh gases are delivered through a single dual-acting, spring-loaded poppet valve located in the center of the cylinder crown. The pressure differential between the cylinder and the intake manifold, and the spring's mechanical characteristics govern the valve opening and closing. The burned charge is exhausted through ports located at the bottom section of each cylinder. This

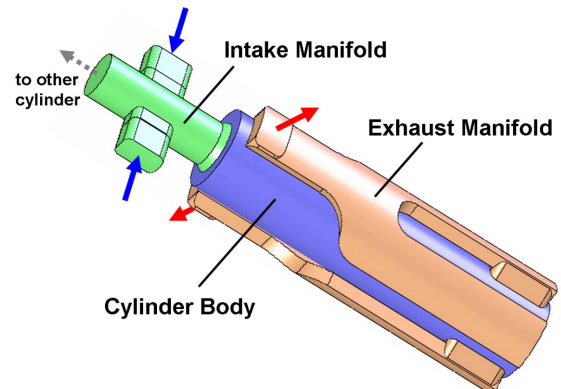


Figure 1 – Preliminary engine configuration – gas-side volume (one side only)

unique scavenging system is termed reverse uniflow and is similar to arrangements proposed in Refs. [11-18].

Figure 1 illustrates a preliminary configuration of the engine, with one combustion chamber depicted. The compressor (power fluid) side is not considered in this report. The initial design is being configured to employ upstream fuel mixing; packaging requirements limit the use of direct in-cylinder injection. The reverse uniflow arrangement provides a novel means of charge replacement, however, achieving effective scavenging at high speed (the piston's small mass will result in an operating frequency near 200Hz (12,000RPM)) without the use of manifold directed porting, as is employed in many 2S arrangements, may be challenging. One opportunity to affect the in-cylinder dynamics may be through the use of a swirl-generating manifold arrangement, similar to those used for small bore, direct injection (DI) engines [19-24]. This option will be briefly discussed later in this paper. Ignition of the charge could be achieved through a glow plug (as discussed in Refs. [25,26]), or by using homogeneous charge compression ignition (HCCI), both of which do not require a controlled/timed ignition source. The gas transfer process is critical towards achieving adequate charge preparation and engine operation, while minimizing fuel loss and unacceptable pollutant emissions.

The objective of this work was to begin the development of the engine with particular focus on the scavenging

system. A commercial computational fluid dynamics (CFD) software suite, STAR-CD/ESICE was used as the primary tool. Global scavenging parameters including the scavenging efficiency (η_{sc}) and delivery ratio (Λ) are used as metrics to evaluate the performance of the initial designs. Visualization of the in-cylinder charge motion through the gas transfer and compression processes allows sources of short-circuiting and the mixture quality near the start of combustion (SOC) to be evaluated. Based on the results, modifications of the initial design will be suggested.

BACKGROUND

Free piston engines have received considerable attention in recent years due to mechanical advantages, improved powerplant efficiency (especially for platforms which don't require shaft power), and increased capabilities of control systems. Examples of recent free piston thrusts can be found in Refs. [1-10]. Free piston designs generally require two-stroke charge replacement because it is difficult/expensive to drive the piston(s) in a pumping mode without mechanical linkages.

Computational tools have frequently been used in the development of charging systems for modern engines, including 2S engines [27-36]. Possible methods include 1D gas dynamic models, multi-dimensional Navier-Stokes models, and partially or fully coupled 1D-3D software. Gas dynamic models enable the effects of pressure waves through the manifold system to be investigated. These models are particularly useful for geometries where the piping configuration is a constraint for the design, and for designs operating over a large frequency-power space, where tuning can be challenging. Multi-dimensional models allow the in-cylinder flow fields to be investigated. These are advantageous when developing new scavenging and combustion chamber designs, especially where the relation between charging and short-circuiting is not well established. Multi-dimensional CFD models however, can be time consuming to set up and costly to run; adequate mesh resolution can be difficult to achieve. In addition, these models rely on the application of boundary conditions (BC) at the inlets and exits of the computational domain which may or may not be realistic. A critical value is the time varying manifold pressure; experimental, computed and simplified isobaric conditions have historically been used. Coupled 1D-3D approaches integrate these models' capabilities and provide a more comprehensive (and accurate) evaluation of a particular design. However, more parameters, and foreknowledge of the design configuration must be available.

Experimental gas transfer, or scavenging rigs have sometimes been used in conjunction with computational tools [37-44]. Single-shot and steady flow rigs can allow the charging performance to be evaluated under engine simulated conditions. Single-shot devices include the dynamic nature of the piston, but cycle-to-cycle coupling

is lost and liquid-phase fluids are often utilized to improve the visualization capabilities through the scavenging process. Steady flow rigs can allow the induction system to be parameterized under constant pressure-drop, constant-lift operating conditions. For these apparatuses the flow and/or friction coefficients are often reported, sometimes with accompanying flow visualization. Entrainment regions and other potential problem areas can sometimes be spotted.

A combined numerical and experimental approach is being pursued in the development of this small-scale engine. Multi-dimensional simulations have been conducted due to the novelty of the reverse uniflow arrangement; these are expected to indicate the potential of the proposed configuration. This report describes the CFD set up and some initial simulations; the unique flow characteristics of the scavenging system are discussed. A companion report describes a steady flow rig that has been constructed to evaluate various swirl-generating intake manifold configurations [45].

The remainder of this paper is organized as follows. Details of the computational setup and simulation are provided in the next section with sample CFD results presented after that. The capabilities of the initial configuration and the potential of the reverse uniflow scavenging arrangement are then discussed with possibilities for future design modifications listed after that.

COMPUTATIONAL SETUP

The commercial software suite, STAR-CD/ESICE was used as the primary tool [46]. A 0D free piston dynamics (FPD) code was first used to estimate the initial port and valve configuration (i.e., size and timings). The FPD code was developed previously to characterize the operation of a free piston electrical generator [1]; it couples the kinematics of the free piston to the pressure dynamics of an internal combustion engine. The initial port/valve size and timings were incorporated into the CFD mesh and simulation. The computational domain was constructed using the ESICE and PROAM modules of the STAR-CD suite. The mesh included the entire cylinder volume and sections of the intake and exhaust manifolds; 300,000 hexahedral and tetrahedral cells were used. A straight intake manifold was employed for the initial simulations, and only one of the combustion chambers was modeled. The mesh density was refined in regions of large temperature, pressure, and momentum gradients, including near the intake valve seat and exhaust ports. An image of the mesh at bottom dead center (BDC) is illustrated in Figure 2; the surface mesh and a cutaway section of the cylinder volume are shown here. Details of the engine specifications used for these simulations are listed in Table 1. A large bore to stroke ratio is used to minimize possible interference during the free piston engine's operation.

In the operating engine the spring-activated, dual-acting valve will utilize a stubbed geometry, as shown in Figure

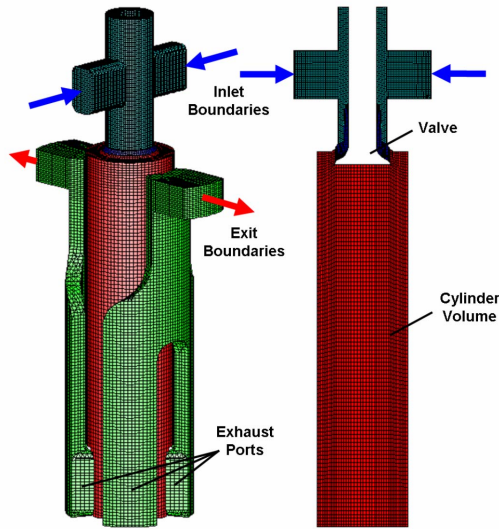


Figure 2 – Computational domain; piston at BDC

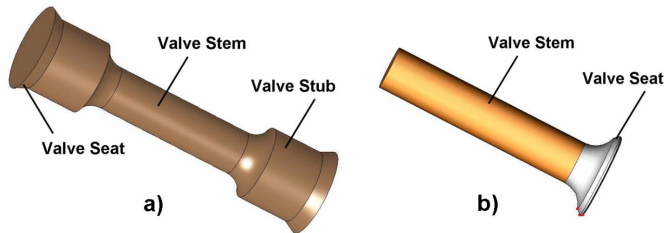


Figure 3 – a) Dual-acting stubbed valve and b) valve geometry used for CFD simulations

Table 1: Engine specifications

Bore [mm]	15
Stroke [mm]	62
TDC volume [mm ³]	540
Trapped volume [mm ³]	9,220
Swept volume [mm ³]	10,860
Compression Ratio	17:1
Operating frequency [Hz / RPM]	200 / 12,000
Intake equivalence ratio	0.75
Inlet pressure [bar]	1.5, nominal
Exit pressure [bar]	1.0
Number of intake valves	1
Intake valve diameter [mm]	8
Intake valve lift [mm]	2.4
Number of exhaust ports	4
Exhaust port height [mm]	11.4
Exhaust port width [mm]	8.9
EPO – EPC [CAD]	118 – 242
IVO – IVC [CAD]	130 – 230

3a. This will allow the valve to close without completely seating; seating will occur when the pressure differential across the valve actuates the spring located within the valve stem. The spring will be designed to open and close the valve based on the desired timings and the working cylinder pressures within the opposing

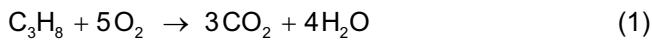
combustion chambers. The design of this component is beyond the scope of this paper. For this initial series of simulations however a conventional type poppet valve geometry (shown in Fig. 3b) and lift history was used; future CFD runs expect to incorporate the stubbed geometry into the mesh, though this will require modifications to the STAR-CD/ESICE software.

The simulations were computed over a number of engine cycles, from 3 to 7, depending on the initial conditions used, in order for the calculations to become consistent. This is due to the significant coupling that is present in 2S engines (relative to 4S devices); the blowdown conditions (at the end of the expansion processes) drive the scavenging process which in turn affects the heat release on the next cycle, and then the expansion & blowdown conditions, etc. The piston motion was defined by a conventional crankshaft-driven trajectory, even though this configuration will be for a free piston. Future computations expect to incorporate a coupled free piston profile, meaning the trajectory will be dynamically determined based on the in-cylinder and power fluid conditions. Compared to a free piston profile however, the scavenging time (absolute) is about 20% greater for the crankshaft-driven trajectory, due to the lower deceleration / acceleration rates of the piston near BDC – this means that the intake and exhaust timings, to allow for adequate charge replacement, will need to be increased for more realistic piston trajectories. The flow characteristics for this geometry however, should be quite similar for the different piston trajectories (under the constraint that the scavenging times are similar, as discussed in Ref. [5]).

Constant pressure conditions were applied at the inlet and exit boundaries; these BC's can be improved for future runs towards more realistic simulations, such as when the initial manifold design is completed. With this modification the port/valve timings may need to be adjusted to achieve comparable scavenging performance. The standard $k-\epsilon$ turbulence model was employed with no-slip and law-of-the wall conditions applied on all solid surfaces. The temperatures of the piston, head, valve and cylinder wall were all set to 500K for the runs. The fluid solver uses the PISO algorithm with an average of 5 corrector stages at each iteration; an under-relaxation factor of 0.8 was used for pressure correction. All flow variables (except density) were solved using an upwind differencing scheme; central differencing was used for density. A time split method was used for the chemistry solver due to the stiffness of the PDE's.

For this investigation, the combustion process was computed using a homogeneous reactor model (in order to simulate HCCI combustion), meaning that within each computational cell in the cylinder the heat release process is governed by kinetic reactions; sub-grid scale inhomogeneities and turbulent mixing are not taken into account. The rate of heat release is determined by solving a set of coupled kinetic equations. For these runs a single, irreversible reaction was employed using

propane as the fuel; future work can use more detailed mechanisms. Equations 1 and 2 present the global reaction mechanism and the rate equation used. Table 2 lists the rate constants for Eq. (2). These are based on parameters suggested by Westbrook and Dryer [47], but were modified due to limitations with StarCD's solver. Large mass fraction exponential values (m, n in Eq. (2)) can lead to high stiffness of the simulation which causes the code to crash under dynamic conditions (i.e., transient engine processes with significant in-cylinder stratification of temperature and species). The mass fraction exponentials and the pre-exponential constant were adjusted to achieve stable simulations while maintaining ignition delays close to the original parameters. (For the operating conditions here (equivalence ratio~0.75, P_{ig} ~40bar, T_{ig} ~1000K) the ignition delay is ~40% longer, which results in a shift in SOC by about +20CAD at 12,000RPM.)



$$\frac{d[C_3H_8]}{dt} = -A \exp(-E_a/R_u T) [C_3H_8]^m [O_2]^n \quad (2)$$

Table 2: Rate constants for propane oxidation

A	28.5E+11 [(mol/cm ³)/s]
E _a	125.5 [kJ/mol]
m	0.75
n	1.00

The simulations were initialized at 115 crank angle degrees (CAD), 3 CAD before exhaust port opening (EPO); this allowed the simulations to converge on a consistent (cycle-to-cycle) solution quicker than if the initial starting point were set to anywhere else in the cycle. The port and valve timings are listed in Table 1. The initial runs were simulated using an operating frequency of 200Hz (12,000RPM); this is based on the results from the 0D FPD code (a piston mass of 12g, and an electrical-type resistance to piston motion was assumed – the power fluid compression dynamics were not modeled in the FPD code).

SCAVENGING PARAMETERS

The scavenging efficiency and delivery ratio are primary metrics used for evaluation of 2S engine systems; these are defined in Equations (3) and (4), respectively. The trapping efficiency is also evaluated and this is defined in Eq. (5).

$$\eta_{sc} = \frac{\text{mass of delivered charge retained}}{\text{mass of trapped cylinder charge}} \quad (3)$$

$$\Lambda = \frac{\text{mass of delivered mixture per cycle}}{\text{reference mass}} \quad (4)$$

$$\eta_{tr} = \frac{\text{mass of delivered charge retained}}{\text{mass of delivered charge}} \quad (5)$$

For these simulations, the scavenging parameters were calculated by tracking the fuel flow through the computational mesh. Boundary interfaces at the intake valve curtain and the exhaust port were used to determine inflow to and outflow from the cylinder volume. Since it was assumed that all of the fuel will be consumed during the combustion cycle, this approach allows relatively easy computation of the scavenging parameters. Previous studies have used a switching algorithm where 'fresh charge' and 'residual charge' are stored as different species with 'fresh charge' switched to 'residual charge' after the ports and valves close [5, 48]. This is difficult to implement in a commercial code like STAR-CD/ESICE and thus the fuel tracking method was employed. This method is similar to scavenging measurements in operating engines (where a reactant or product specie like O₂ or CO₂ is used [49-54]), and it assumes that the fresh fuel & air mixture mixes and diffuses at similar rates. The calculation for η_{sc} is presented in Eq. (6) for reference; $y_{fuel,in}$ is the mass fraction of fuel in the intake stream, for propane / air with an intake equivalence ratio of 0.75 this is 0.0458.

$$\eta_{sc} = \left(1 + y_{fuel,in}^{-1}\right) \frac{(m_{fuel})_{cyl}}{(m_{total})_{cyl}} \quad (6)$$

The reference mass used in Eq. (4) is taken as the trapped cylinder volume multiplied by the ambient (i.e., atmospheric) density as opposed to the inlet density.

COMPUTATIONAL RESULTS

The computed charging dynamics and engine operating behavior are discussed in this section; computation times averaged about 6 days (at each operating point) with the calculations distributed over 8 processors per run. A sweep of charging pressures from 1.2 to 2.1bar was used to achieve various delivery ratios for the reverse-uniflow configuration. Figure 4 plots the scavenging and trapping efficiencies versus delivery ratio for four cases, using intake pressures of 1.2, 1.5, 1.8 and 2.1bars and exhaust pressure of 1.0bar. Also included in this plot are the theoretical limits for the perfect displacement and perfect mixing models for reference; the target operating range for the engine is highlighted as well.

As can be seen, the scavenging performance for the initial configuration of the engine lies between the two theoretical curves, as might be expected. It is slightly reduced from the performance expected from a conventional uniflow engine, and lower than the design target. The typical rolloff in η_{sc} is seen at higher delivery ratios as entrainment and short-circuiting issues become problematic. Future work will attempt to shift the scavenging curves towards the target region.

Figure 5 plots the intake and exhaust mass flow rates for the four cases; positive mass flow indicates flow into the cylinder while negative flow rates indicate charge leaving the cylinder. A number of features are evident from the curves in this plot. First, it can be seen that the blowdown process is more intense for the higher charging pressure runs. This is due mainly to the higher scavenging efficiencies achieved for these cases which results in higher combustion pressures and higher ensuing blowdown pressures. The pressure at EPC for each of the four cases is nearly identical (as seen in Fig. 6), indicating that the variation in blowdown pressure is primarily a function of the concentration of the fuel trapped in the cylinder.

Next in Fig. 5, the slight back flow that develops through the cylinder as the intake valve is opened can be seen. This flow reversal is due to the higher pressure of the cylinder charge relative to the intake manifold and results in a delay of delivery of the fresh charge to the cylinder. It is interesting to note that the flow dynamics (i.e., intake and exhaust flow rates) are quite similar across the three higher pressure cases during the backflow process. Future runs should work to adjust the valve / port timing to ensure adequate blowdown before IVO.

Finally in Fig. 5 it can be seen that through a good portion of the charging process (167-206CAD) the intake and exhaust flow rates are nearly steady. This characteristic indicates a restriction in the flow path, with this possibly being in the valve region. Indeed, as seen in the companion experimental report [45], the thick stem of the spring-loaded valve constrains the flow geometrically after a non-dimensional lift (L/D_v) of 0.17. The lift used for these simulations was 2.4mm, which corresponds to a non-dimensional value of 0.3. Through a good portion of the valve lift therefore, there is no benefit to higher lifts.

Figures 6 and 7 plot the average cylinder pressure and average temperature versus cylinder volume, respectively, on a log-log scale for the four different cases. The compression ratio across these runs were set to 17:1; this was done in order to ensure ignition across each of the startup engine cycles, even though over-compression after combustion (during operation) can lead to significant heat loss from the charge. A number of features are evident in these figures. First, the pressure history through much of the compression stroke for each of the runs is nearly identical. Departure of the traces occurs as the ignition timing is shifted due to the differences in charge temperature (as seen in Fig. 7). During expansion the 2.1bar charging case has the highest pressure due to the greatest heat released for this case, as discussed earlier. The shift in average charge temperature between the runs explains the differences in SOC.

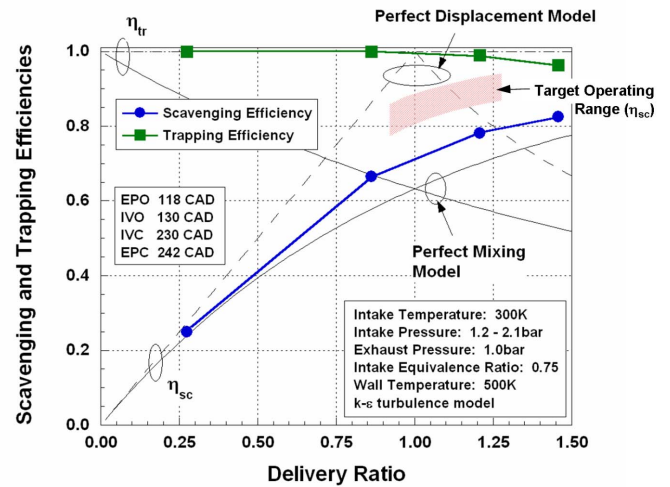


Figure 4 – Computed scavenging and trapping efficiencies over a range of delivery ratios using the initial configuration with charging pressures of 1.2, 1.5, 1.8 and 2.1bar, and an intake equivalence ratio of 0.75.

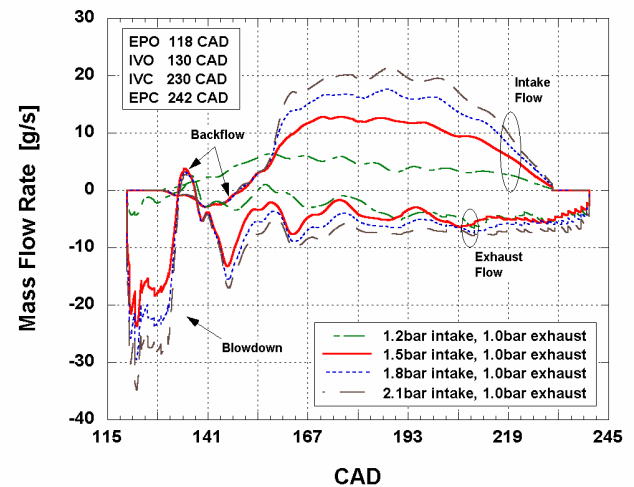


Figure 5 – Computed intake / exhaust mass flow rates for the initial configuration with charging pressures of 1.2, 1.5, 1.8 and 2.1bar, and an intake equivalence ratio of 0.75.

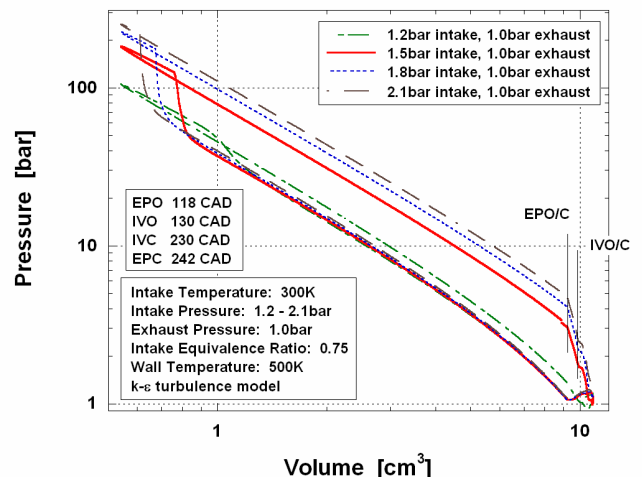


Figure 6– Log pressure versus log volume for initial configuration with charging pressures of 1.2, 1.5, 1.8 and 2.1bar, and an intake equivalence ratio of 0.75.

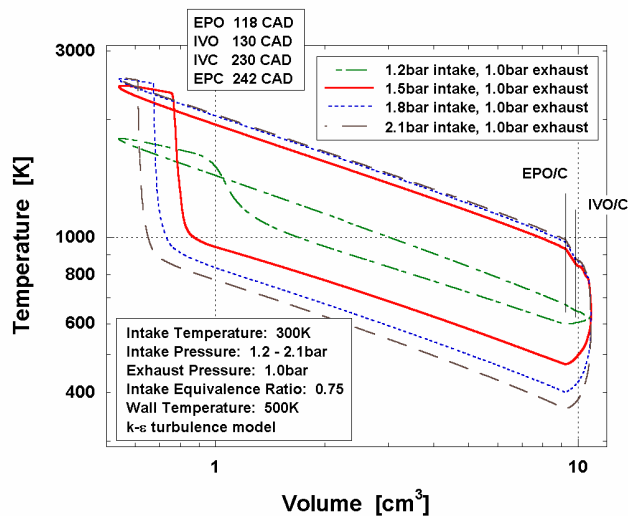


Figure 7– Log temperature versus log volume for initial configuration with charging pressures of 1.2, 1.5, 1.8 and 2.1bar, and an intake equivalence ratio of 0.75.

Finally from Figs. 6 & 7, it can be seen that there is significant curvature present through both the compression and expansion strokes (during the port/valve closure period), indicating that there is significant heat transfer to / from the trapped cylinder charge, with this due to the large surface area to volume ratio present in this small configuration. The issue of heat loss can also be seen in the counter-clockwise looping behavior of the pressure and temperature traces near TDC.

Figure 8 illustrates additional results from the simulations where spatial distributions of the fuel mass fraction are plotted through the scavenging process for the 1.5bar charging pressure case. A cut plane is imaged parallel to the intake flow, and colors on the plane indicate the strength of the in-cylinder charge; these run from 0.0 (blue) to 0.0458 (red), or an equivalence ratio from 0-0.75. Times of 145CAD through 245CAD are presented. Through these images the issue of backflow into the intake manifold can be seen. Recirculation and entrainment below the valve are also visible, as is the incomplete penetration of the fresh charge into the cylinder (which limits the cylinder flushing). Finally, it appears that a toroidal vortex is generated along the cylinder wall during the intake process; this affects the ensuing in-cylinder dynamics through the compression process (as seen in Fig. 10).

Figure 9 accompanies Fig. 8 where the temperature contours along the same cut planes are illustrated through the scavenging process. The issues of backflow, recirculation / entrainment, incomplete penetration and toroidal vortex generation are also visible here.

Figure 10 illustrates the development of the in-cylinder flow during the compression process, towards the combustion / heat release event. Here the same cut-plane is used though the temperature scale has been modified from Fig. 9. It can be seen that during the compression process, the toroidal vortex rotating along

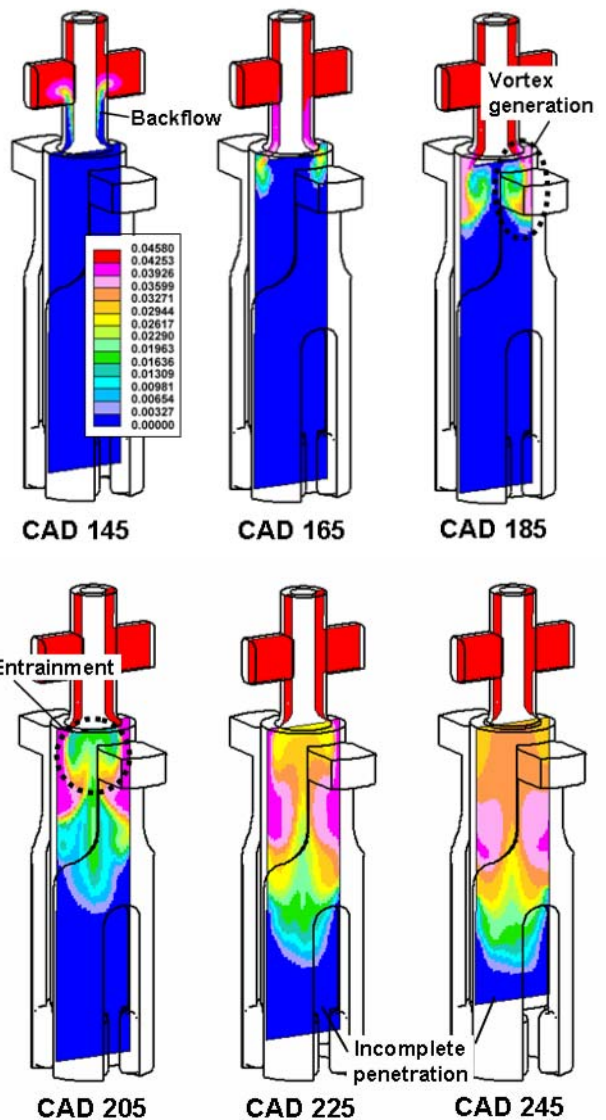


Figure 8 – Contours of predicted fuel mass fraction through the scavenging process, imaged on a cut plane parallel to the intake flow, for a nominal charging pressure of 1.5bar and an equivalence ratio of 0.75.

the wall works to bring the high temperature, residual gases from the piston crown towards the valve region. This hot core of entrained residuals & fresh charge is the first part of the mixture to ignite, with the rest of the charge following it. Pressure waves are then initiated from this region.

SUMMARY AND CONCLUSIONS

The operating cycle of a novel, reverse-uniflow 2S engine has been simulated using the commercial software package, StarCD/ESICE. For an initial configuration which includes a single, dual-acting, centrally located intake valve, and four circumferentially located exhaust ports, the effects of the scavenging process on the in-cylinder dynamics have been illustrated. Due to non-optimal port and valve timings a fairly low scavenging efficiencies were realized; backflow into the intake manifold delayed the introduction of fresh

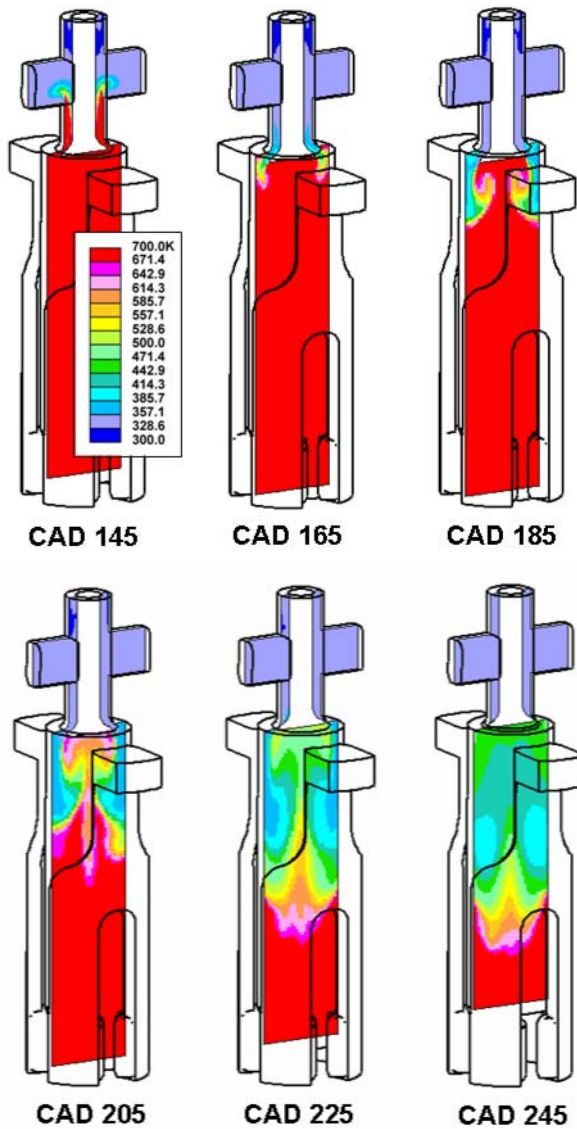


Figure 9 – Contours of predicted temperature through the scavenging process, imaged on a cut plane parallel to the intake flow, for a nominal charging pressure of 1.5bar and an equivalence ratio of 0.75

charge into the cylinder, and there is a significant flow restriction due to the wide, non-conventional valve stem geometry. The centrally-located intake valve, tightly packaged into the cylinder head results in a large entrainment region beneath the valve, and the generation of a toroidal vortex along the cylinder wall. The vortex can work to transport the hot residual gases stratified near the piston crown, toward the cylinder head during the compression process.

These non-optimal flow characteristics limit the potential of the scavenging process and should possibly be addressed in the further development of the engine. Future work will include variations in the engine operating frequency, valve lift/timing, and port height/width in attempt to improve the scavenging performance towards the design goals. In addition, manifold-directioning (e.g., see Ref. [45]) may enable modification or control of the in-cylinder flow patterns which could address the valve recirculation problem.

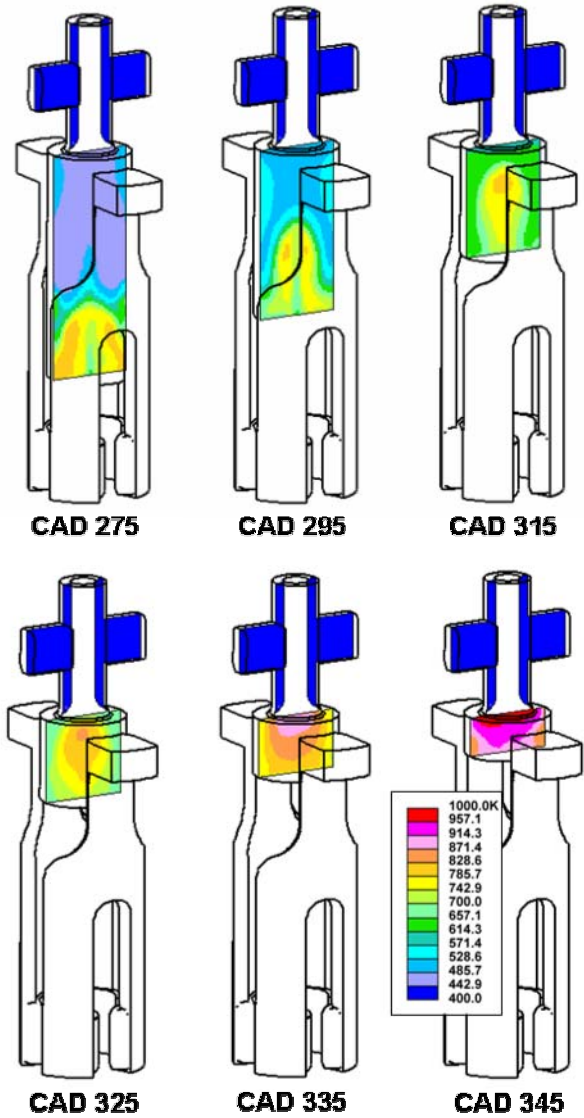


Figure 10 – Contours of predicted temperature through the compression process, imaged on a cut plane parallel to the intake flow, for a nominal charging pressure of 1.5bar and an equivalence ratio of 0.75; note the change in scale from Fig. 8.

ACKNOWLEDGMENTS

Simulations were conducted on Marquette's Cluster Computing Facility with equipment funding provided through NSF grant CTS-0521602.

REFERENCES

1. Goldsborough, S. and Van Blarigan, P., "A numerical study of a free piston IC engine operating on homogeneous charge compression ignition," SAE Technical Paper 1999-01-0619.
2. Goertz, M. and Ping, L., "Free Piston Engine: Its Application and Optimization," SAE Technical Paper 2000-01-0996.
3. Tikkanen, S., Lammila, M., Herranen, M. And Vilenius, M., "First Cycles of the Dual Hydraulic Free Piston Engine," SAE Technical Paper 2000-01-2546, 2000.

4. Larmi, M., Isaksson, S., Tikkanen, S. And Lammila, M., "Performance Simulation of a Compression Ignition Free Piston Engine," SAE Technical Paper 2001-01-0280, 2001.
5. Goldsborough, S. and Van Blarigan, P., "Optimizing the Scavenging System for a Two-Stroke Cycle Free Piston Engine for High Efficiency and Low Emissions: A Computational Approach", SAE Technical Paper 2003-01-0001, 2003.
6. Fredriksson, J. and Denbratt, I., "Simulation of a Two-Stroke Free Piston Engine," SAE Technical Paper 2004-01-1871, 2004.
7. Kleemann, A.P., Dabadie, J.-C. And Heriot, S., "Computational Design Studies for a High-Efficiency and Low-Emissions Free Piston Engine Prototype," SAE Technical Paper 2004-01-2928, 2004.
8. Caresana, F., Comodi, G. and Pelagalli, L., "Design Approach for a Two-Stroke Free Piston Engine for Electric Power Generation," SAE 2004-32-0037, SAE Technical Paper, 2004.
9. Brusstar, M., Gray Jr., C., Jaffri, K., McCarthy, P. And Pomerleau, M., "Design, Development and Testing of Multi-Cylinder Hydraulic Free-Piston Engines," SAE Technical Paper 2005-01-1167.
10. Fredriksson, J., Bergman, M., Golovitchev, V. And Denbratt, I., "Modeling the Effect of Injection Schedule Change on Free Piston Engine Operation," SAE Technical Paper 2006-01-0449, 2006.
11. Moriyoshi, Y., Kukuchi, K., Morikawa, K. and Takimoto, H., "Numerical Analysis of Mixture Preparation in a Reverse Uniflow-Type Two-Stroke Gasoline DI Engine," SAE Technical Paper 2001-01-1815, 2001.
12. Moriyoshi, Y., Kukuchi, K., Morikawa, K. and Takimoto, H., "Development and Evaluation of a Reverse Uniflow-Type Two-Stroke Gasoline DI Engine," SAE Technical Paper 2001-01-1839, 2001.
13. Moriyoshi, Y., Morikawa, K. and Takimoto, H., "Analysis of Mixture Formation Process in a Reverse Uniflow-Type Two-Stroke Gasoline DI Engine," SAE Technical Paper 2002-32-1774, 2002.
14. Moriyoshi, Y., Arai, M., Katsuta, J., Morikawa, K., "Performance Tests of Reverse-Uniflow-Type, Two-Stroke Direct Injection Gasoline Engine," SAE Technical Paper 2004-32-0040, 2004.
15. Moriyoshi, Y., Arai, M., Katsuta, J., Morikawa, K., "Performance Analysis of Reverse-Uniflow-Type, Two-Stroke Direct Injection Gasoline Engine," SAE Technical Paper 2004-08-0088, 2004.
16. Ohlmann, D., Reynolds, S. and Ciccarelli, G., "Development of a Novel Uniflow-Scavenged, Two-Stroke GDI Engine," SAE Technical Paper 2006-01-0187, 2006.
17. Rival, D. and Ciccarelli, G., "Evaluation of Scavenging Performance in a Novel Two-Stroke GDI Engine," SAE Technical Paper 2006-01-0446, 2006.
18. Oliver, P., Reynolds, S. and Ciccarelli, G., "Flowbench Calibration of a Numerical Model for a Novel Uniflow-Scavenged, Two-Stroke GDI Engine," SAE Technical Paper 2006-01-3268, 2006.
19. Kawashima, J., Ogawa, H. and Tsuru, Y., "Research on a Variable Swirl Intake Port for 4-Valve High-Speed DI Diesel Engines," SAE Technical Paper 982680, 1998.
20. Li, Y., Li, L., Xu, J., Gong, X., Liu, S. and Xu, S., "Effects of Combination and Orientation of Intake Ports on Swirl Motion in Four-Valve DI Diesel Engines," SAE Technical Paper 2000-01-1823, 2000.
21. Page, V.J. and Blundell, G.D., "The application of design of experiments and CFD to the optimization of a fully parametric helical port design," SAE Technical Paper 2000-04-0367, 2000.
22. Shuliang, L., Yufeng, L., Zhenzhong, Z., Lihong, R., Haodong, Z, Jie, S. and Songfang, Z., "An Investigation of the Effects of Manufacturing Deviations of Helical Inlet Port on the Flow Characteristics of DI Diesel Engines," SAE Technical Paper 2001-01-3507, 2001.
23. Pastor, J.V., Margo, X., Gil, A. and Donayre, J.C., "A Methodology to Estimate the Swirl Number at TDC in DI Diesel Engines: Through the Combination of CFD and Steady Flow Rig Results," SAE Technical Paper 2004-01-1876, 2004.
24. Kulkarni, Y., Mone, M., Desai, A., Markandeya, S., Nayak, N., Aghav, Y., Sohi, N.S. and Dani, A.D., "Optimization of Inlet Port Performance on Emission Compliance of Naturally Aspirated DI Diesel Engine," SAE Technical Paper 2005-26-010, 2005.
25. Raine, R. R. and Thorwarth, H., "Performance and Combustion Characteristics of a Glow-Ignition Two-Stroke Engine," SAE Technical Paper 2004-01-1407, 2004.
26. Manente, V., Tunestål, P., Johansson, B., "A Study of a Glow Plug Ignition Engine by Chemiluminescence Images," SAE Technical Paper 2007-01-1884, 2007.
27. Payri, F., Galindo, J., Climent, H., Pastor, J.M. and Gaia, C., "Optimisation of the Scavenging and Injection Processes of an Air-Assisted Direct Fuel Injection 50 cc. 2-Stroke S.I. Engine by Means of Modelling," SAE Technical Paper 2001-01-1814, 2001.
28. Gustafsson, R.U.K., Blair, G.P., Jonsson, B.I.R., "Reducing exhaust emissions and increasing power output using a tuned exhaust pipe on a two-stroke engine," SAE Technical Paper 2001-01-1853, 2001.
29. Chiatti, G. and Chiavola, O., "Integrated numerical-experimental method in high-speed 2T gasoline engine design and refinement," SAE Technical Paper 2001-01-1855, 2001.
30. Riegler, U.G. and Bargende, M., "Direct coupled 1D/3D-CFD-computation (GT-Power/Star-CD) of the flow in the switchover intake system of an 8-cylinder SI engine with external exhaust gas recirculation," SAE Technical Paper 2002-01-0901, 2002.
31. Zeng, Y. and Strauss, S., "Modelling of scavenging and plugging in a twin-cylinder, two-stroke engine using CFD," SAE Technical Paper 2003-32-0020, 2003.
32. Zeng, Y., Strauss, S., Lucier, P. and Craft, T., "Predicting and Optimizing Two-Stroke Engine Performance Using Multidimensional CFD," SAE Technical Paper 2004-32-0039, 2004.
33. Bozza, F. and Gimelli, A., "A Comprehensive 1D model for the simulation of a small-size, two-stroke SI engine," SAE Technical Paper 2004-01-0999, 2004.

34. Onorati, A., Cerri, T., Ceccarani, M. and Cacciatore, D., "Experimental Analysis and 1D Thermo-Fluid Dynamic Simulation of a High-Performance Lamborghini V10 S.I. Engine," SAE Technical Paper 2005-24-081, 2005.
35. Rothbauer, R.J., Almbauer, R.A., Schmidt, S.P., Margelik, R.H. and Glinsner, K., "A Multidimensional Interface for the Predictive CFD Simulation of the 2-Stroke Engine," SAE Technical Paper 2006-32-0059, 2006.
36. Fleck, B., Fleck, R., Kee, R.J., Hu, X., Foley, L., Yavuz, I., "CFD Simulation and Validation of the Scavenging Process in a 125cc 2-Stroke Racing Engine," SAE Technical Paper 2006-32-0061, 2006.
37. Kee, R.K., McEntee, P.T., Blair, G.P., Fickenscher, T., Hölzer, J., Douglas, R., "Validation of two-stroke engine simulation by a transient test method," SAE Technical Paper 978510, 1997.
38. McElligott, S., Douglas, R., Kenney, R.G. and Glover, S., "An assessment of a stratified scavenging process applied to a loop-scavenged, two-stroke engine," SAE Technical Paper 1999-01-3272, 1999.
39. Millo, F., Gallone, A., and Mallamo, A., "Experimental and Computational Analysis of a Tuned Exhaust System for a Small Two-Stroke Engine," SAE Technical Paper 1999-01-3329, 1999.
40. Kuwahara, K., Watanabe, T., Tanada, H., Ueda, K., Ando, H. and Yokoe, M., "Intake-Port Design for Mitsubishi GDI Engine to Realize Distinctive In-Cylinder Flow and High Charge Coefficient," SAE Technical Paper 2000-01-2801, 2000.
41. Torregrosa, A.J., Galindo, J., Payri, R., Climent, H. and Gaia, C., "Modeling the exhaust system in two-stroke small engines," SAE Technical Paper 2001-01-3317, 2001.
42. Li, Y., Zhao, H., Leach, B., Ma, T. and Ladommatos, N., "Optimisation of In-Cylinder Flow for Fuel Stratification in a Three-Valve Twin-Spark-Plug SI Engine," SAE Technical Paper 2003-01-0635, 2003.
43. Stuecke, P., Egbers, C. and Geyer, W., "Visualization of the flow inside the transfer channels of small two-stroke cylinders," SAE Technical Paper 2003-32-0008, 2003.
44. Algieri, A., Bova, S. and De Bartolo, C., "Global Flow Characterization of a Four Cylinder Spark Ignition Engine during the Intake Phase," SAE Technical Paper 2005-24-075, 2005.
45. Johnson, M.V. and Goldsborough, S.S., "Constructing a small-scale flow rig for swirl studies of a single-valve, reverse uniflow 2S engine," SAE Paper 2008-01-0609, 2008.
46. Star-CD User Guide, Version 3.26, CD-Adapco, 2005.
47. Westbrook, C.K. and Dryer, F.L., "Simplified Reaction Mechanisms for the Oxidation of Hydrocarbon Fuels in Flames," Combustion Science and Technology, 27:31-43, 1981.
48. Zhu, Y.-X., Savonen, C., Johnson, N.L. and Amsden, A.A., "Three-dimensional computations of the scavenging process in an opposed-piston engine," SAE Paper 941899, 1994.
49. Isigami, S., Tanaka, Y. and Tamari, M., "The Trapping Efficiency Measurement of Two Stroke Cycle Diesel Engien by Tracer Gas Method," Bulletin of JSME, 6:524-531, 1963.
50. Huber, E.W., "Measuring the Trapping Efficiency of Internal Combustion Engines Through Continuous Exhaust Gas Analysis," SAE Technical Paper 710144, 1971.
51. Nuti, M. and Martorano, L., "Short-Circuiting Ratio Evaluation in the Scavenging of Two-Stroke S.I. Engines," SAE Technical Paper 850177, 1985.
52. Hashimoto, E., Tottori, T. and Terata, S., "Scavenging Performance Measurements of High speed Two-Stroke Engines," SAE Technical Paper 850182, 1985.
53. Chiatti, G. and Chiavola, O., "Scavenging Efficiency and Combustion Performance in 2T Gasoline Engine," SAE Technical Paper 2003-32-0030, 2003.
54. Foudray, H.Z. and Ghandhi, J.B., "Scavenging Measurements in a Direct-Injection Two-Stroke Engine," SAE Technical Paper 2003-32-0081, 2003.

CONTACT

S. Scott Goldsborough
Department of Mechanical Engineering
Marquette University
Milwaukee, Wisconsin 53201-1881
Scott.Goldsborough@mu.edu